

High Resolution Polarimetry With a Balloon-Borne Telescope: The Flare Genesis Experiment

P. N. Bernasconi, D. M. Rust, G. A. Murphy, H. A. C. Eaton
*JHU/Applied Physics Laboratory, 11100 Johns Hopkins Road,
Laurel, MD 20723-6099, USA*

Abstract. The Flare Genesis Experiment consists of an 80 cm balloon-borne Ritchey-Chrétien telescope which will provide 0."2 spatial resolution vector magnetograms. Wavelength and polarization state selection are accomplished respectively with a lithium niobate Fabry-Perot etalon, and a liquid crystal modulator. This paper describes recent modifications to the experiment, mainly to the optics and to the pointing system. The aim is to reach in the next flight the diffraction limit of the telescope and to assure 0."1 pointing accuracy during the time needed to record a full set of vector polarimetric measurements (typically 10 seconds). The telescope optics have been extensively tuned and tested at the McMath-Pierce Solar Telescope at Kitt Peak during winter and spring 1998, while the pointing system has been tested in Palestine (Texas) in August/September 1998. Some test results are presented.

1. Introduction

There is a consensus in the solar physics community that to better understand the origin and evolution of solar activity greatly improved magnetic field observations are needed. Higher resolution, greater stability during observations and long runs without interruptions are expected to reveal key features of the magnetic energy buildup and release needed to explain solar activity.

The major limiting factor in ground-based observations is the thermal turbulence of the Earth's atmosphere (seeing) that distorts the wavefront of the light coming from the Sun. In recent years various techniques have been developed to overcome this problem. One method is to calculate the wavefront distortion that occurred during the data recording and to subsequently reconstruct the undistorted images (speckle interferometry and phase diversity). Another way is to compensate the wavefront distortion in real-time by means of adaptive or active optical systems. Finally, the best way to eliminate the seeing degradation effects is to place a telescope above the Earth's atmosphere. This can be done either by installing the telescope in a spacecraft or by using a stratospheric balloon.

The Applied Physics Laboratory (APL) of the Johns Hopkins University has launched an effort to fly a balloon-borne 80 cm aperture telescope in the Antarctic stratosphere. It will be able to image and measure the vector magnetic field in the solar photosphere and chromosphere over long periods of time with

an unprecedented spatial resolution of $0.''2$.

The primary scientific objective of the FGE is to understand the mechanisms which lead the fibrous magnetic fields at the solar surface to erupt in solar flares. In addition the FGE is well suited to study the evolution of the magnetic structure and helicity (twist of field lines) of active regions and filaments, to investigate the properties of small-scale magnetic elements and their contribution to solar luminosity variations and coronal heating, and to study solar oscillations at the smallest scales.

2. The Instrument

The FGE characteristics and capabilities have already been extensively described and discussed in Rust et al. (1996, 1993), and Murphy et al. (1996). Here we will just summarize its main features.

The telescope is an 80 cm Ritchey-Chrétien with an F/1.5 primary mirror made of ULE and honeycombed to a weight of just 50 kg. Its support and spider arms are made of graphite-epoxy and provide high thermal stability over a wide temperature range. The secondary mirror is made of single-crystal silicon which provides optimum heat transfer with minimal thermal distortion. The heat is removed from the secondary by means of a set of copper heat straps that connect the back of the secondary to the spider arm heat shields that also operate as radiators. In order to reduce the heat load on the primary mirror, a “heat dump” mirror was installed in front of it (see M3 in Fig. 1), which passes the light only from a small region on the Sun while the rest is reflected out the front of the telescope. The FGE telescope at floating altitude (~ 32 km) can achieve its diffraction-limited spatial resolution of $0.''2$.

Attached to the back of the mirror cell is a 1.2 m diameter pressure vessel (OPV, see Fig. 1), where most of the post focus optics is housed, as well as some of the electronics. The main post focus instrument is a vector magnetograph, whose major components are a polarization analyzer composed by two liquid crystal modulators and a linear polarizer, a tunable 75 mm diameter lithium niobate Fabry-Perot etalon (Rust 1994), and a 10 bit 1532×1024 pixels CCD camera. The temperature controlled polarization analyzer is located directly behind the prime focus to minimize instrumental polarization (see Fig. 1). The Fabry-Perot filter has a passband of about $160 \text{ m}\text{\AA}$ and, in conjunction with a series of narrow-band blocking filters ($\sim 1.5 \text{ \AA}$ passband), it can be tuned to any of the four spectral lines: 6563 \AA ($\text{H}\alpha$, $g = 1.045$), 6122 \AA (CaI , $g = 1.75$), 6302 \AA (FeI , $g = 2.5$), or 6249 \AA (continuum). The image scale at the CCD camera is $0.''1$ per pixel which gives a field of view of about $150'' \times 100''$. The vector magnetograph will provide time series of vector magnetograms at various wavelengths, and also of vector velocity and intensity in the photosphere and chromosphere. Depending upon on the tradeoffs in data processing, the magnetic sensitivity will be $1 - 10 \text{ G}$ for the longitudinal component and $50 - 100 \text{ G}$ for the transversal component. The on-board tape recorder is provided with 9 tape cassettes, each capable of storing 6000 images, for a resulting data storage capability of 54000 images.

To maintain an image at the FGE focal plane stabilized down to the level of $0.''1$ during the exposures, despite the oscillation of the gondola, we adopted an

Image Motion Compensator (IMC). Its components are a Lateral Effect Diode (LED), installed at the focus of the pointing telescope which gives the pointing errors in elevation and azimuth with a sensitivity of $0.''05$, and an agile tip-tilt mirror mounted right after the polarization analyzer where an image of the pupil is formed (see Fig. 1). The mirror is moved to compensate for the pointing errors as read by the LED.

The telescope is mounted to the gondola frame on its elevation axis which goes through the center of gravity of the telescope. It is moved on this axis by a motor whose stator is connected to the gondola and its rotor to the telescope. The pointing in azimuth is achieved by turning the entire gondola using a Reaction Wheel (RW) mounted on the top of the structure. The gondola is rotated by spinning up or down the RW while its motor is connected to the gondola (see Sec. 4.2).

The electronics is housed in four pressure vessels mounted on a mezzanine above the telescope. The vessels which are maintained near 20° C, allow commercial-grade components to be used, thereby considerably lowering the costs.

3. First flight

From January 7 to 26, 1996, FGE had its first Antarctic flight, one of the longest balloon flights yet in Antarctica. The pointing system remained locked on the Sun for the entire flight. With the exception of the first 18 hours of flight, when the telescope was in the line-of-sight, and during an 11 hours flight beneath the payload with an LC-130 aircraft on January 10, the telescope operated autonomously. For the entire flight a $30''$ solar target tracking was maintained.

On January 26, the FGE payload came down in an area inaccessible to large cargo aircraft. However, a team did reach the site in a small airplane and did recover the data tapes. The rest of the payload had to remain on the Antarctic ice until December 1996, when, with the aid of the U. S. and French Antarctic programs, we recovered the gondola and the telescope. The overall condition of the payload was good. The solar panels were destroyed during the hard landing, and the gondola aluminum frame was bent, but the telescope itself was in good condition. At APL the telescope tube and mirror cell were carefully measured and no damages or warping were detected. We started then to rebuild the payload for a second flight.

The analysis of the flight data revealed that the image resolution in the first flight was limited to only about $1''$. However, the major FGE systems performed as expected and we feel that the basic engineering approach, in particular the mechanical, thermal and electrical system design, is sound.

4. Design modifications and test results

Even though the first flight of FGE proved its feasibility, the scientific return was relatively small for mainly two reasons. First, because of a problem in focusing and alignment the image resolution was considerably lower than the expected $0.''2$. Second, the pointing was not accurate enough to enable the Image Motion Compensator to stabilize the image jitter down to $0.''1$ during the exposures. In

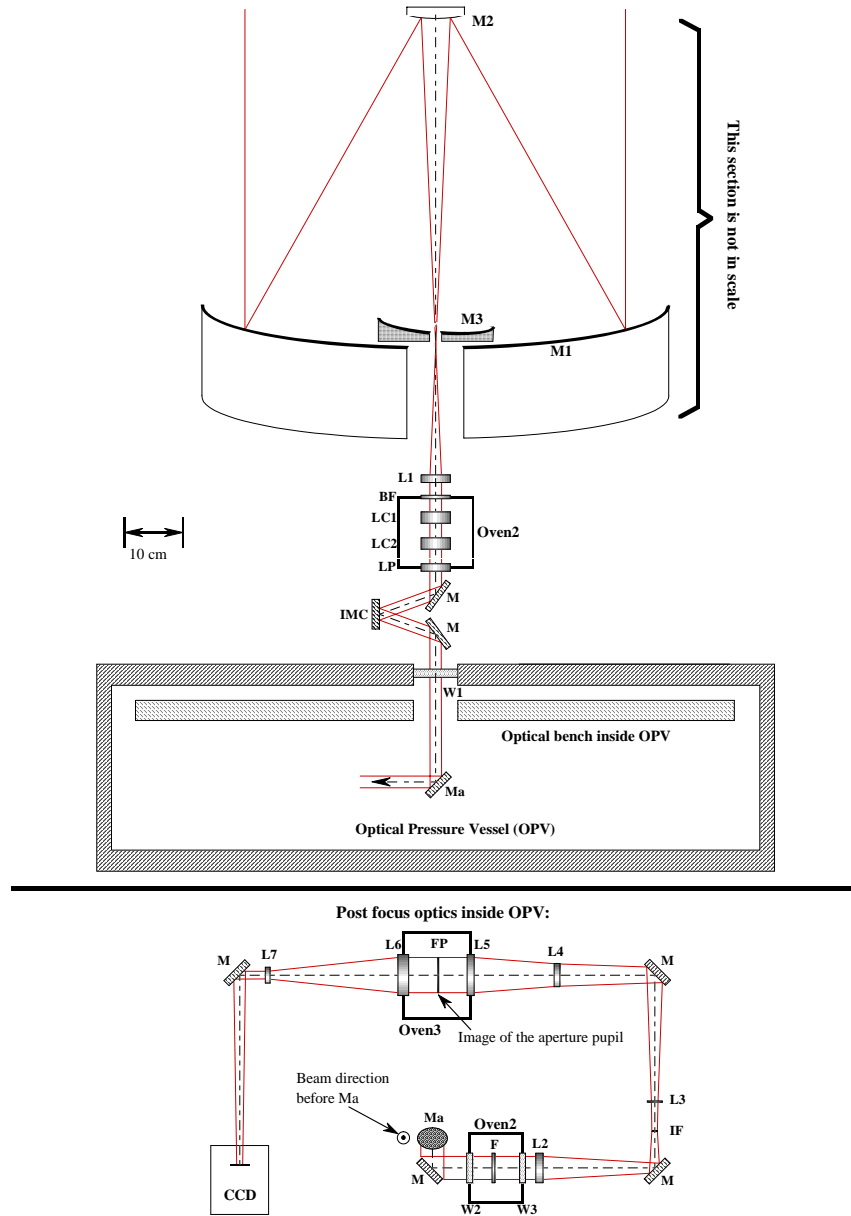


Figure 1. Scheme of the FGE optics: M = beamfolding mirror, M1 = primary mirror (ULE, $\phi = 80$ cm, F/1.5), M2 = secondary mirror (silicon), M3 = heat dump mirror, L1-L7 = objective lenses, BF = broadband filter (500 \AA passband centered at $\lambda = 6328 \text{ \AA}$), LC1-2 = liquid crystal modulators, LP = linear polarizer, IMC = image motion compensator mirror, W1 = OPV window, Ma = first beamfolding mirror inside the OPV, W2-3 = flat windows of Oven2, F = narrow-band filter (0.16 \AA passband, a filter wheel is used to switch between different filters), IF = intermediate image focus, FP = Fabry-Perot etalon.

the next two sections we will describe the modification we made to improve the FGE performance.

4.1. Optics

The original optical design was very complex (see Murphy et al. 1996), and it was very difficult to exactly align all the optics. Therefore we decided to significantly simplify the optical path. In Fig. 1 the new optical path is shown. In particular, we removed the Target Selector Telescope (TST), which was mounted parallel to the main telescope and formed a full disk image also on the CCD camera inside the OPV. The images from the TST were analyzed by the computer on-board to determine regions of interest on the Sun to direct the observation program while out of contact with the ground. Both, the main telescope beam and the TST beam were feeding the same detector, and it turned out to be very hard to correctly coalign these two beams. So we decided to eliminate the TST. During the next flight the coordinates of the regions of interest will be transmitted to the on-board computer via a low speed radio link making use of the Inmarsat or NOAA/Argos data packets (see Murphy et al. 1996).

In order to test the new FGE optics with sunlight, the telescope was shipped to Kitt Peak (Arizona) and installed at the NOAO/NSO McMath-Pierce Solar Telescope. The latter was used to feed the FGE telescope with a stable, 1.5 m diameter parallel solar beam. In this way we could separate the problems of pointing from those of achieving optimum optical performance. On June 21, 1998, we had good seeing conditions and we were able to record the filtergram shown in Fig. 2, and the longitudinal magnetogram of the same active region displayed in Fig. 3. We believe that the filtergram in Fig. 2 is seeing-limited. Other interferometric tests confirm that the telescope and the focal plane optics are operating near the diffraction limit of $0.''2$.

The longitudinal magnetogram was obtained by combining the two polarization images $I + V$ and $I - V$ recorded consecutively with the Fabry-Perot passband sitting in the blue wing of the Ca I 6122 Å line. The magnetogram is not very accurate since the two images have been taken with a time interval of a few seconds between each other, and due to the seeing, they are not exactly the same (no destretching procedure was applied to the filtergrams). In flight there will be no seeing and this problem will disappear. In addition many consecutive polarization measurements will be added together in the post flight data processing, significantly increasing the magnetic sensitivity.

4.2. Pointing system

Even though the rms azimuthal pointing error during the first flight was $\sim 30''$ (in elevation the rms error was about a factor 2 smaller) we encountered periodic pointing disturbances with error peaks up to $100''$ (see the top diagram in Fig. 5). These spikes were too large to be compensated by the IMC mirror. The origin of the disturbances was found in the Momentum Transfer Unit (MTU), which is used to transfer excess angular momentum to the balloon.

The left image of Fig. 4 shows a scheme of the MTU employed during the first flight. The MTU was originally designed by the Harvard/Smithsonian Center for Astrophysics. All the weight of the gondola is resting on the thrust bearing, transferring the weight to the central shaft which is connected to the

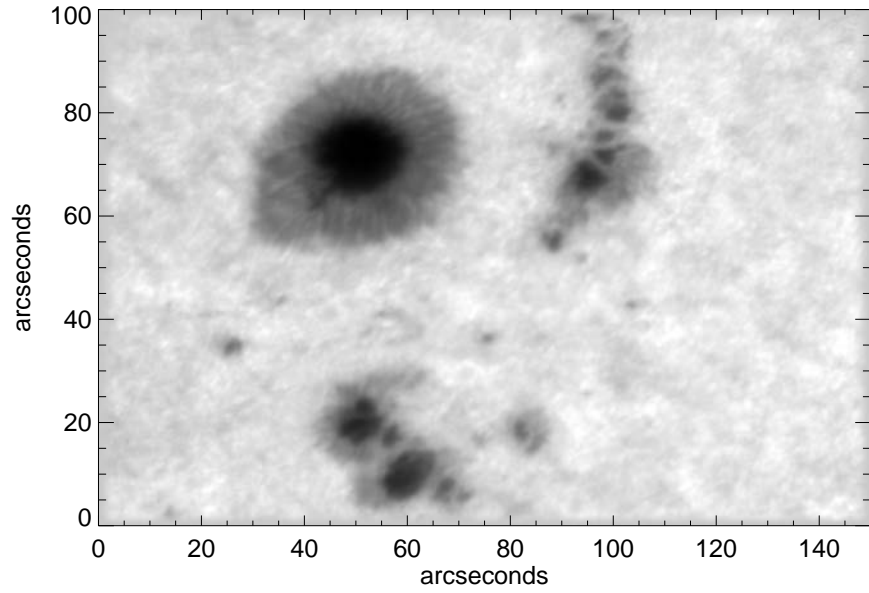


Figure 2. Filtergram of a sunspot group located at $\theta = 37.5^\circ$ in the NW solar quadrant, recorded on June 21, 1998 with the FGE CCD camera. The Fabry-Perot passband was positioned in the core of the CaI 6122 Å line.

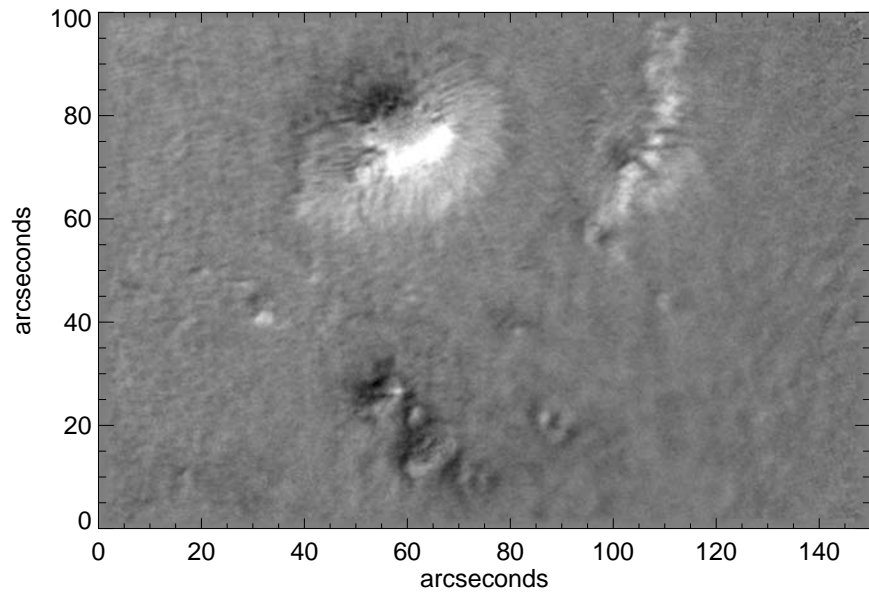


Figure 3. Longitudinal magnetogram of the same active region shown in Fig. 2. It represents the degree of circular polarization as recorded in the blue wing of the CaI 6122 Å line. White (black) means field pointing towards (away from) the observer.

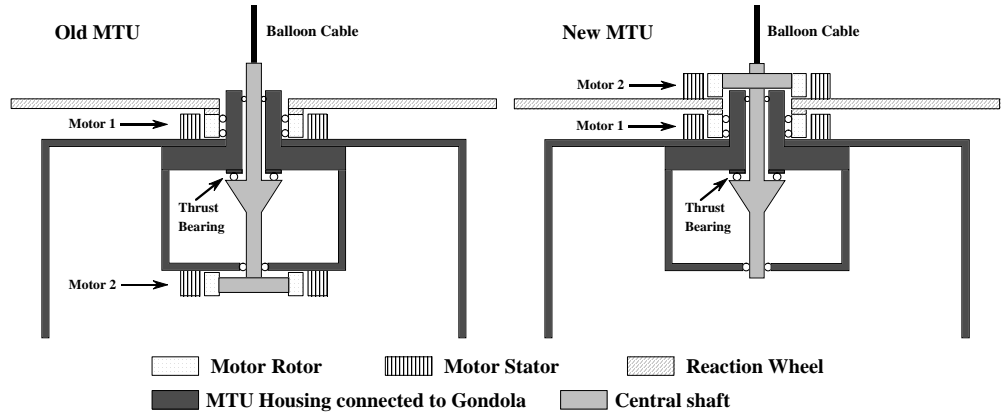


Figure 4. Simplified diagrams of the Momentum Transfer Unit used during the first flight (left) and the improved present one (right).

balloon. Motor 1 has its rotor connected to the RW and its stator to the gondola. When a current is applied to Motor 1 a torque is produced and gondola and RW are accelerated, spinning in opposite directions. In this way the telescope can be steered in azimuth. If the RW starts to rotate at high speed (above 1 revolution per second) it becomes difficult to apply large torques that would speed it further, and the servo system will not be able to provide the necessary steering torques. To slow it down, an additional torque opposite to the spin must be applied. This additional torque cannot be transferred to the gondola since this would compromise the pointing. It must be transferred to the balloon. This is achieved with the aid of another motor (Motor 2) whose stator is connected to the gondola and whose rotor is connected to the central shaft. Motor 2 generates a torque exactly opposite to the one needed to slow the wheel down. This is transferred to the balloon cable. However, despite all efforts, it was no possible to match exactly the torques produced by the two motors. Consequently, an error torque is applied to the gondola during momentum dump. The top diagram in Fig. 5 shows that the high disturbances occur when momentum is transferred from the RW to the balloon cable.

To reduce this effect as much as possible we designed a new MTU, which is shown in the right image of Fig. 4. Motor 2 has its rotor still connected to the central shaft, but its stator is now connected directly to the RW instead of the MTU housing. In this configuration only Motor 1 can apply torques to the gondola. Motor 2 will operate as before whenever the RW needs to be slowed down.

We tested the new MTU at the NASA Scientific Balloon Facility (Texas) by hanging the gondola from a crane and by letting the telescope point at the Sun. The azimuthal pointing errors are shown in the bottom diagram in Fig. 5. The improvement in pointing performance is evident. Even though we must stress that the test conditions on the ground are much less difficult than the ones during the flight. Now the rms error in azimuth is below $2''$, and the disturbances during momentum dumps are considerably smaller and briefer. This kind of pointing errors can be removed by our IMC.

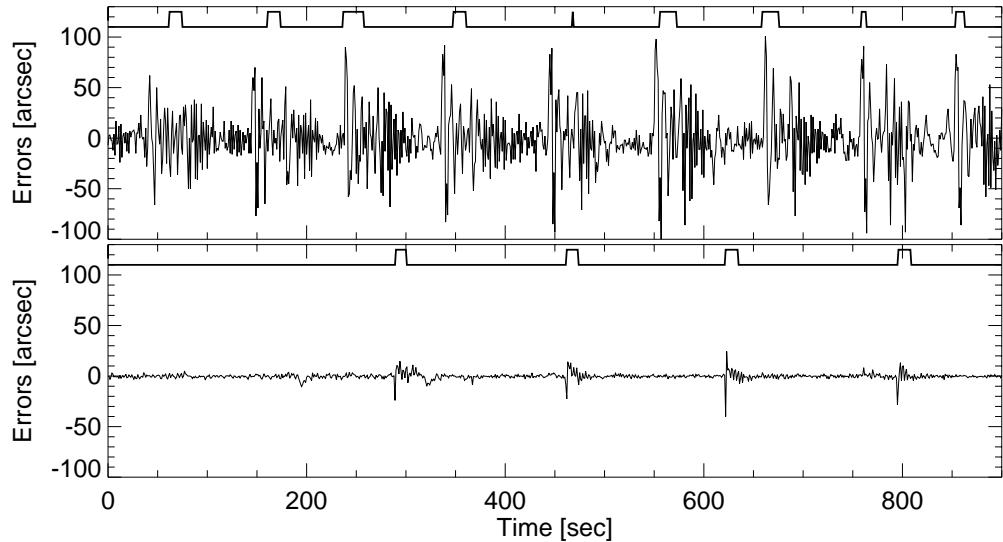


Figure 5. Azimuthal pointing errors in a typical time frame during the first flight (top), and during the ground tests with the new MTU in nearly ideal environmental conditions (bottom). The blips in the thick lines at the top of each diagram show the times when momentum was transferred from the reaction wheel to the balloon cable.

5. Conclusions

The FGE is a system for obtaining uninterrupted high resolution solar observations. The experience gained from the first flight led us to simplify the optical system and modify the pointing system. The next flight is scheduled for December 1999 during the peak of the solar activity in the present cycle. More information and the status of the project can be obtained by visiting our Web site: <http://sd-www.jhuapl.edu/FlareGenesis>.

Acknowledgments. We thank NOAO/National Solar Observatory for their help and for giving us the chance to test our telescope at their facilities at Kitt Peak. This work was supported by NSF under grant OPP-9615073 and NASA under grant NAG5-4955.

References

- Murphy, G. A., Rust, D. M., Strohbahn, K., Eaton, H. A. C., Keil, S. L., Keller, C. U., and Wiborg, P. 1996, Proc. SPIE, 2804, 141
- Rust, D. M. 1994, Optical Eng., 33, 3342
- Rust, D. M., Hayes, J. R., Lohr, D. A., Murphy, G. A., and Strohbahn, K. 1993, Johns Hopkins APL Tech. Digest, 14, 358
- Rust, D. M., Murphy, G. A., Strohbahn, K., and Keller, C. U. 1996, Sol. Phys., 164, 403